Supplementary Materials: Exploring Manufacturing Process and Degradation Products of Gilt and Painted Leather

Morena Iorio, Valerio Graziani, Sergio Lins, Stefano Ridolfi, Paolo Branchini, Andrea Fabbri, Gabriel Ingo, Gabriella Di Carlo and Luca Tortora

Leather support and Silver leaf

MA-XRF elemental maps

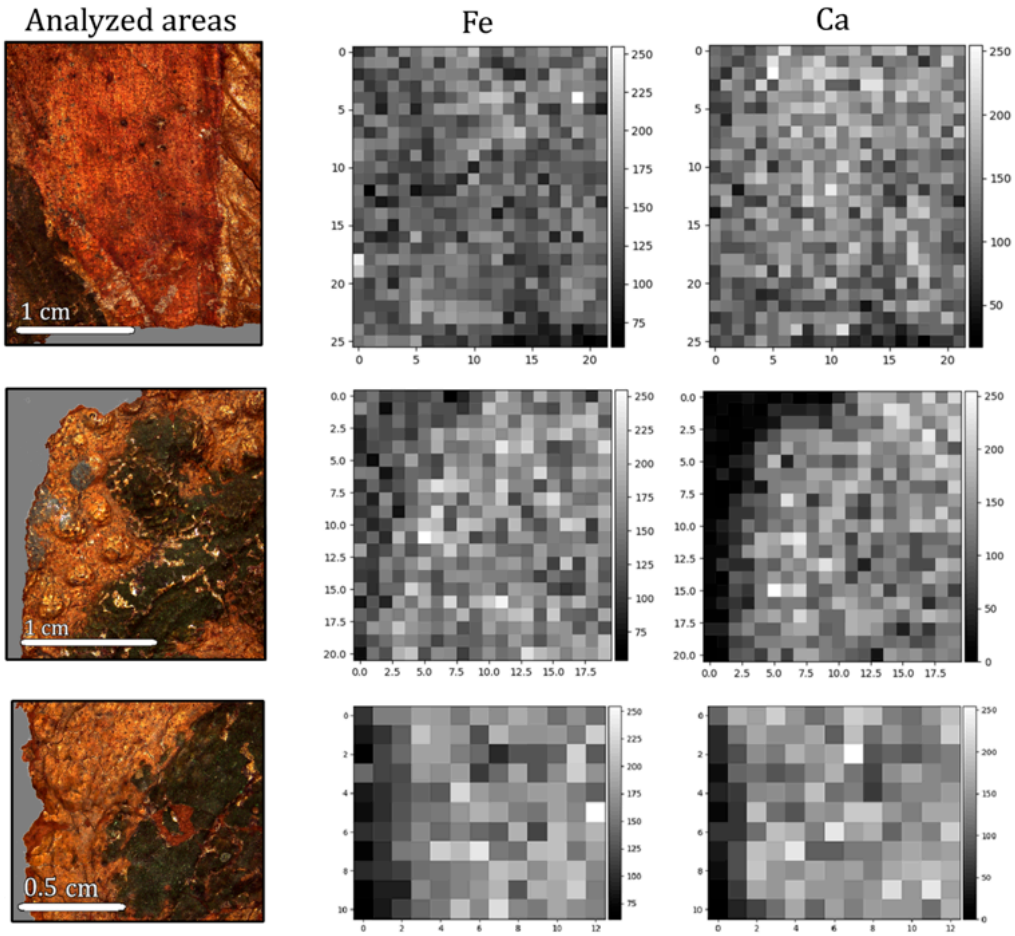

Figure S1. From top to bottom: MA-XRF elemental maps of Ca and Fe from sample 1, sample 2 (left area) and sample 2 (right area).

ToF-SIMS peak attributions

Peak and spectra related to clusters of silver (Ag^+, m/z 107; Ag_2^+, m/z 214; Ag_3^+ m/z 321; Ag_5^+ m/z 534), silver oxides ($Ag_3O_2^+$, m/z 353; $Ag_5O_2^+$, m/z 567), silver chlorides (Ag_2Cl^+, m/z 249; $Ag_3Cl_2^+$, m/z 391; Ag_4Cl^+, m/z 463) and silver sulfides (AgS^+, m/z 139; Ag_2S^+, m/z 246; Ag_3S^+, m/z 353) are shown in Figure S2.

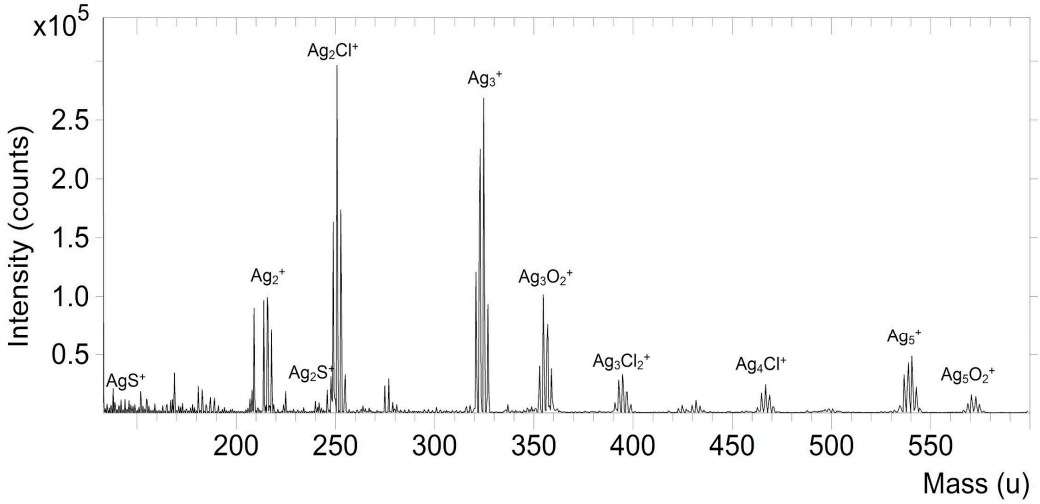

Figure S2. Part of positive ion mass spectra extracted from the silver leaf and showing clusters of silver (Ag^+, m/z 107; Ag_2^+, m/z 214; Ag_3^+ m/z 321; Ag_5^+ m/z 534), silver oxides ($Ag_3O_2^+$, m/z 353; $Ag_5O_2^+$, m/z 567), silver chlorides (Ag_2Cl^+, m/z 249; $Ag_3Cl_2^+$, m/z 391; Ag_4Cl^+, m/z 463) and silver sulfides (AgS^+, m/z 139; Ag_2S^+, m/z 246; Ag_3S^+, m/z 353).

Gold Varnish

MA-XRF elemental maps

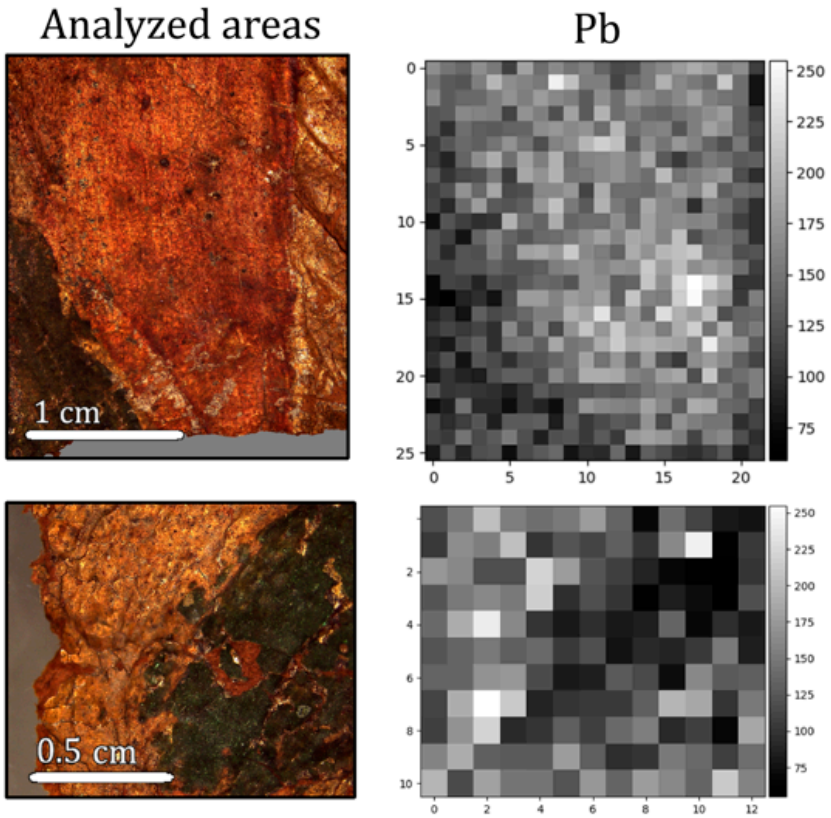

Figure S3. MA-XRF elemental maps of Pb obtained from leather samples 1 and 2 (from top to bottom).

FTIR bands

Figure S4 shows recognizable spectral features at 2920 cm^{-1} (ν[C-H]), 2851 cm^{-1} (ν[C-H]), 1704 cm^{-1} (ν[C=O]), 1629 cm^{-1} (ν[C=O], in amide I), 1542 cm^{-1} (ν[C-N] and in-plane bending of N-H, both from amide

II), 1459 cm^{-1} (bending of C-H and ν_3[C-O] from CO_3^{-2} group), 1417 cm^{-1} (ν_3[C-O] from CO_3^{-2} group), 1316 cm^{-1} (ν[C-O]), 1159 cm^{-1} (ν[C-O]), 1099 cm^{-1} (ν[C-O] from hydroxyl-bonding carbon and ν_1[C-O] from CO_3^{-2} group), 1031 cm^{-1} ($\rho[CH_3]$), 1006 cm^{-1} ($\rho[CH_3]$), 874 cm^{-1} (ν_2[C-O]), 780 cm^{-1} ($\rho[CH_2]$).

Spectral features for sample 3 showing the presence of an additional compound (Figure 4c) are: a group of three peaks at around 2900 cm^{-1} related to ν[C-H] (which is more intense if compared to the couple present in the spectrum from sample 1), a sharp peak at 1701 cm^{-1} related to ν[C=O] of carboxylic group and a couple of peaks at 1453 and 1383 cm^{-1} related to $\delta[CH_2, CH_3]$ and symmetric bending of $-CH_3$, respectively. The couple of peaks at 1629 and 1542 cm^{-1}, related to amide I and II respectively, is significantly reduced while a new peak centred at 1654 cm^{-1} is recognizable (ν[C=C], non-conjugated).

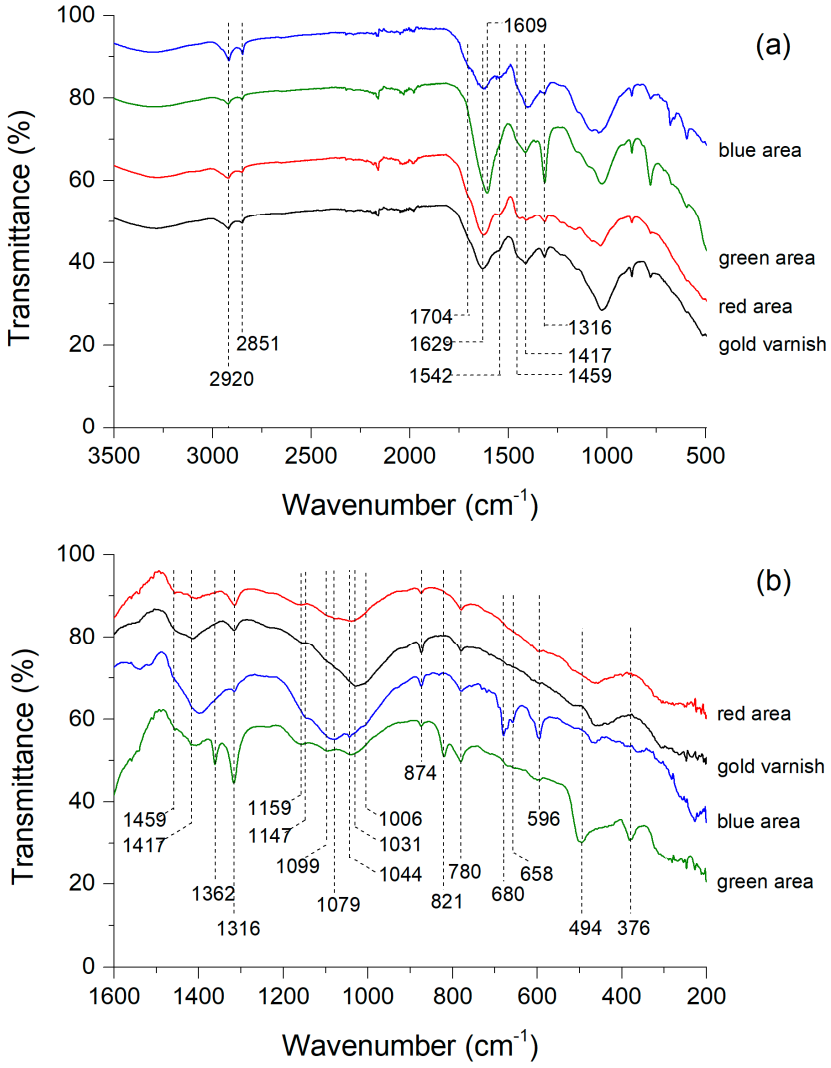

Figure S4. ATR-FTIR spectra of the four coloured areas (a) in the range 3500÷500 cm^{-1} and (b) in the range 1600÷200 cm^{-1}, showing both common and characteristic spectral features.

Blue Area

ToF-SIMS peak attributions

Calcium (Ca^+, m/z 40), calcium-oxygen containing ions ($CaOH^+$, m/z 57) and cluster of lead oxides (Pb_2O^+, m/z 432; $Pb_3O_2^+$, m/z 656 and $Pb_3O_3^+$, m/z 672) and lead hydroxides ($PbOH^+$, m/z 225; $Pb_2O_2H^+$, m/z 450) detected in the blue area are shown in Figure S5 and S6.

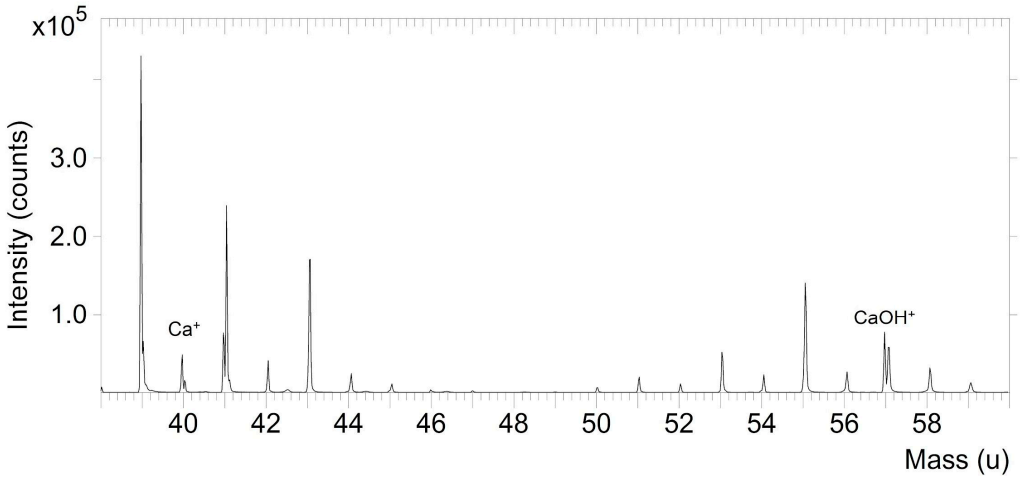

Figure S5. Part of positive ion mass spectra extracted from the blue area and showing calcium (Ca^+, m/z 40) and calcium-oxygen containing ions ($CaOH^+$, m/z 57).

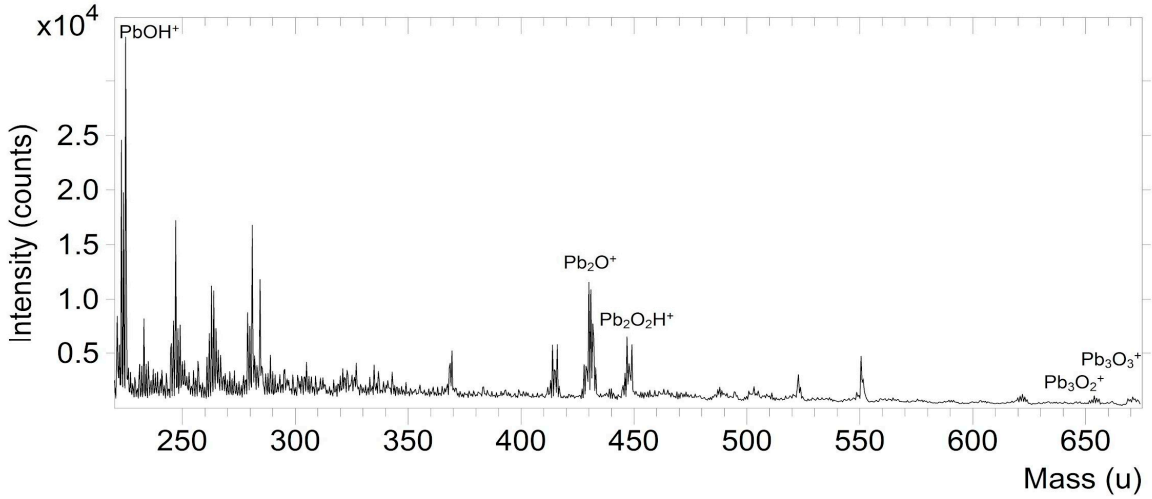

Figure S6. Part of positive ion mass spectra extracted from the blue area and showing cluster of lead oxides (Pb_2O^+, m/z 432; $Pb_3O_2^+$, m/z 656 and $Pb_3O_3^+$, m/z 672) and lead hydroxides ($PbOH^+$, m/z 225; $Pb_2O_2H^+$, m/z 450).

Cluster of lead oxides (PbO^- m/z 224; PbO_2^- m/z 240; Pb_2^- m/z 416; $Pb_2O_2^-$ m/z 447; Pb_3^- m/z 624; Pb_3O^- m/z 640; $Pb_3O_2^-$ m/z 656; $Pb_3O_3^-$ m/z 672, $Pb_3O_3^-$ m/z 672, $Pb_3O_4^-$ m/z 688) and lead hydroxydes ($Pb_2O_3H^-$ m/z 464) detected in negative mode (Figure S7).

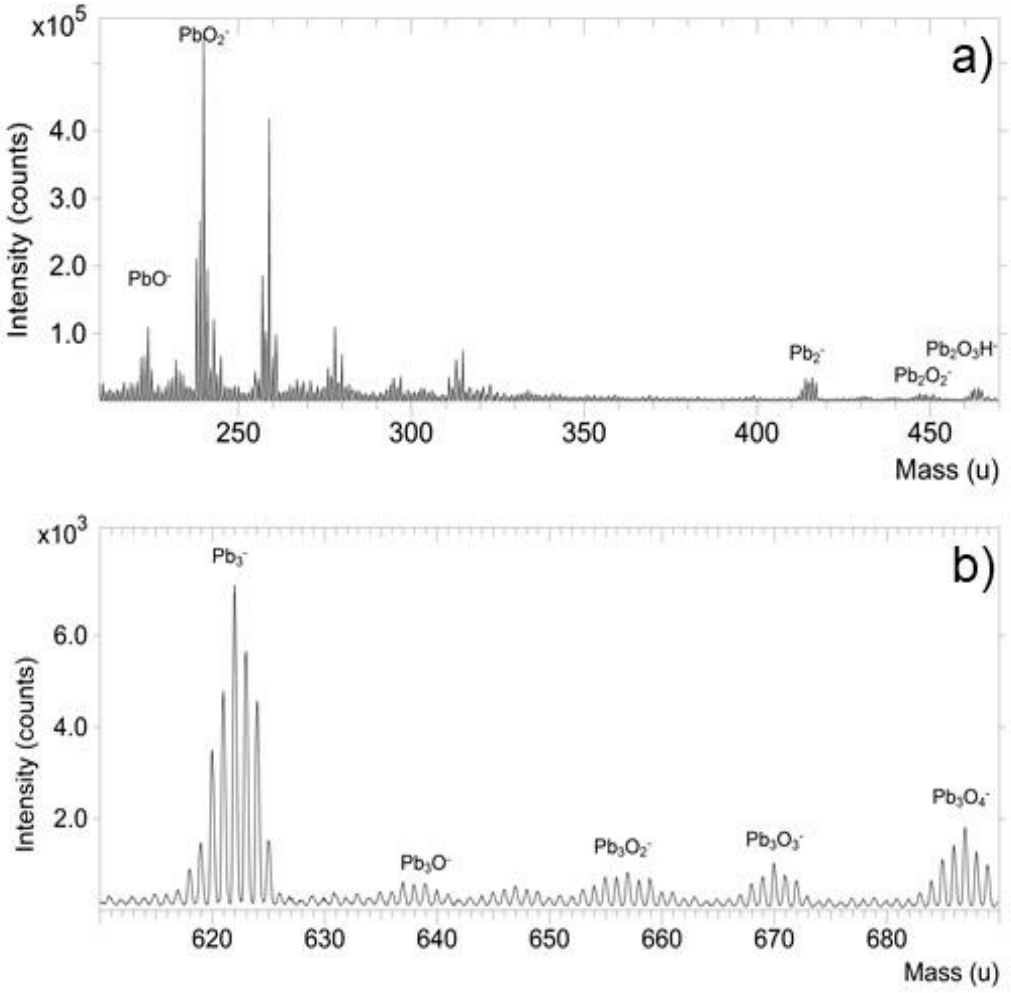

Figure S7. a) Part of negative ion mass spectra (m/z 210-470) extracted from the blue area and showing cluster of lead oxides (PbO^- m/z 224; PbO_2^- m/z 240; Pb_2^- m/z 416; $Pb_2O_2^-$ m/z 447) and lead hydroxydes ($Pb_2O_3H^-$ m/z 464); b) Part of negative ion mass spectra (m/z 610-690) showing cluster of lead oxides (Pb_3^- m/z 624; Pb_3O^- m/z 640; $Pb_3O_2^-$m/z 656; $Pb_3O_3^-$ m/z 672, $Pb_3O_4^-$ m/z 688).

FTIR bands

Figure S4 shows blue area spectral features common to those obtained from gold varnish, with a more intense band of absorption at 1459-1417 cm^{-1} and two very intense shoulders peaked at 1147 cm^{-1} (stretching of -O-P-O^- and ν_3[S=O] from SO_4^{-2} group) and 1099 cm^{-1}. Characteristic features are a peak at 1079 cm^{-1} (assignable to CO_3^{-2} group), a peak at 1044 cm^{-1} (ρ[CH_3] and ν_1[C-O] from CO_3^{-2} group), a couple of intense characteristic peaks at 680 and 658 cm^{-1} (ν_4[C-O] from CO_3^{-2} group and bending of -O-C=O, respectively), a shoulder at 690 cm^{-1} (ν_4[C-O] from CO_3^{-2} group, not marked in Figure S4), a shoulder at 671 cm^{-1} (in-plane bending of N-H from protein and coupled stretching and bending from SO_4^{-2} group, not marked in Figure S4), a shoulder at 616 cm^{-1} (ν_4[S-O] from SO_4^{-2} group, not marked in Figure S4) and a peak at 596 cm^{-1} (bending of -NCO group and ν_4[S-O] from SO_4^{-2} group).